In-Line Jet Mixing of Liquid-Pulp-Fiber Suspensions: Effect of Fiber Properties, Flow Regime, and Jet Penetration

Wisarn Yenjaichon, John R. Grace, Choon Jim Lim, and Chad P.J. Bennington[†]
Dept. of Chemical and Biological Engineering, University of British Columbia, Vancouver, British Columbia, Canada V6T1Z3

DOI 10.1002/aic.13913
Published online September 13, 2012 in Wiley Online Library (wileyonlinelibrary.com).

Mixing effectiveness was determined experimentally for side jet injection into pipe flow for water and pulp suspensions for a range of fiber mass concentrations (0–3.0%), mainstream velocities (0.5–5.0 m/s), and side-stream velocities (1.0–12.7 m/s). The mixing quality was measured in cross-sectional planes along the pipe using electrical resistance tomography and quantified by a modified mixing index, derived from the coefficient of variation of conductivity. Mixing depended strongly on the flow regime and jet penetration. For turbulent flow, the criteria for in-line jet mixing in water are applicable to the mixing in suspensions, with small differences likely due to differences in fiber network strength and influences of fiber-turbulence interactions in modifying turbulent structures in the bulk. When a suspension flows as a plug, however, the mixing differs greatly from that in water, depending on the fiber network strength in the core of the pipe. © 2012 American Institute of Chemical Engineers *AIChE J,* 59: 1420–1430, 2013
Keywords: pulp fiber suspensions, multiphase flow, in-line jet mixing, turbulence, electrical resistance tomography

Introduction

In-line mixers, in which a jet enters mainstream pipe flow from the side, are widely used in the pulp and paper industry. In bleaching processes, for example, various in-line mixers, such as static and high-shear mixers, have been used to provide efficient contacting between chemicals and pulp before tower reactors whose level of mixing is otherwise insufficient. In-line mixers are normally used in conjunction with injectors. Understanding in-line jet mixing behavior is essential as it provides basic concepts and guidance for the design of in-line mixers and for process optimization.

The simplest in-line mixers are tee mixers. A number of experimental studies have been conducted to investigate the mixing of Newtonian fluids after tee mixers, mainly to determine the optimum relationship between jet-to-pipe velocity ratio and diameter ratio for different working fluids and mixing criteria. Details are provided in a previous article.[1] However, for non-Newtonian pulp suspensions few studies have been conducted to study in-line jet mixing behavior and the data are very limited. Bobkowicz and Gauvin[2,3] examined the distribution of hot water in nylon-fiber suspension flow in a vertical flow loop of diameter 50.8 mm. The tracer was injected at the pipe axis, and the radial temperature profile was measured by a temperature probe. The fiber diameters ranged from 20 to 52 μm, their lengths from 0.52 to 1.2 mm, and fiber mass concentration "consistency" from 0.5 to 6.0%. Radial dispersion, determined from the radial intensity of turbulence and eddy diffusion coefficient, increased substantially in the presence of fibers, even when drag reduction occurred. Andersson[4] examined dye dispersion in a standard bleached spruce sulphite pulp flow in a rectangular channel, with turbulence generated by a grid at the inlet of the channel. The suspension concentration ranged from 0 to 5 kg/m^3 and the velocity from 0.13 to 0.83 m/s. Dye dispersion in long-fiber pulp flow decreased with increasing concentration and was less than that in comparable water flow. Luthi[5] qualitatively investigated dispersion of dye injected at the centerline of a 6% pulp suspension flow with a mean velocity of 21.3 m/s. The dye persisted in the core 1.5 m downstream of the injection point, showing that plug flow occurred in the core of the pipe. Luettgen et al.[6] studied the dispersion of saline (KCl) solution in 0.5 wt % hardwood pulp turbulent suspension flow for jet-to-pipe velocity ratios, R, of 0.75 to 12. They found that the KCl dispersed more rapidly in the pulp suspension than in water flow, and this behavior occurred consistently for different velocity ratios. Rewatkar et al.[7] measured the mixing quality of 1% by weight pulp suspensions along the pipe axis downstream of a T-junction based on temperature profiling. They quantified the degree of mixing by the coefficient of variation (CoV). The mixing quality in the pulp suspension flow was significantly less than that for water flow, mainly due to suppression of downstream turbulence.

Suspension rheology plays an important role in determining suspension behavior. The complex rheology of pulp suspensions and its impact on the flow regime, contacts between fibers, floc formation, and dispersion, etc. were summarized by Kerekes.[8] Due to their large aspect ratios (length-to-diameter ratio), fibers collide in rotation and transition in shear flow. Flocculation occurs when closely spaced fibers collide and tangle with each other. Mason[9] defined a condition

[†]*Deceased*
Correspondence concerning this article should be addressed to W. Yenjaichon at wyenjaichon@chbe.ubc.ca.

where fibers were likely to collide in rotation with one fiber in the volume swept out by the length of a single fiber. The corresponding fiber volumetric concentration was called the "critical concentration," given by

$$C_v = 1.5(d/L)^2 \quad (1)$$

where L is the fiber length, and d is the fiber diameter.

Based on this concept, Kerekes et al.[10] defined the propensity for fiber flocculation in terms of a dimensionless number called the "crowding number," defined as the number of fibers in a spherical volume of diameter equal to the fiber length, and given by

$$N_c = \frac{2}{3} C_v (L/d)^2 \quad (2)$$

For pulp fiber suspensions, it is more convenient to base the crowding number on fiber mass concentration, C_m (weight of fibers per weight of suspension, expressed in wt %), and fiber coarseness, ω (weight of fiber wall material for a specific fiber length). Eq. 2 can then be expressed as:

$$N_c \approx \frac{5 C_m L^2}{\omega} \quad (3)$$

Mason's critical concentration clearly corresponds to $N_c = 1$. When $N_c < 1$, each fiber is free on average to rotate without encountering other fibers, and flocculation generally does not occur. Corresponding fiber contacts were characterized as "chance collisions" by Soszynski.[11] Kerekes and Schell[12] showed that N_c can be directly related to the number of contacts per fiber in determining the suspension behavior to form the networks. For $N_c = 60$, there are approximately three contacts per fiber, and fibers become restrained in rotation and locked into a network in a bent configuration.[13] The $1 < N_c < 60$ range was described by Soszynski[11] as one of "forced collisions" between fibers. At higher crowding numbers, fiber mobility decreases significantly, and flocs in the suspension acquire mechanical strength through frictional forces among fibers. Martinez et al.[14] divided the $1 < N_c < 60$ range into two subregimes, separated by $N_c = 16$, defined as the "gel crowding number". For $N_c < 16$, the fibers move freely and the suspension behaves as essentially dilute. For $16 < N_c < 60$, fibers interact with one another and flocculate, but fiber mobility persists. In recent work, Celzard et al.[15] identified a "connectivity threshold" and "rigidity threshold" based on percolation and effective-medium theories, and showed that they correspond to $N_c = 16$ and 60, respectively. The crowding number is a general indicator of the level of fiber contact in flowing systems, helpful in characterizing mixing quality in this study.

Electrical resistance tomography (ERT) is a noninvasive technique, used recently to evaluate mixing in various processes.[16–21] It has also been used to assess the efficiency of in-line mixers in pulp and paper processes. Yenjaichon et al.[22] evaluated the mixing performance of an industrial static mixer in a chlorine dioxide bleaching stage, with injected ClO_2 acting as a tracer. ERT was successfully used to assess the temporal variation of the mixing index, based on the CoV, with the changes in operating conditions including chemical flow rate, suspension flow rate, and fiber mass concentration. Kourunen et al.[23] applied ERT to assess the mixing efficiency of a pilot-scale medium consistency mixer and compared the results with those from temperature measurement. Cold water, air, and steam were used as tracers, with mixing quality again based on the CoV. The softwood pulp suspension mean velocity was approximately 2.1 m/s at $C_m = 10\%$. The mixing quality was found to improve significantly with increasing shear, and ERT results were similar to those from temperature profiling. Yenjaichon et al.[1] investigated the mixing quality of liquid tracer injected into a softwood pulp suspension flow for various fiber mass concentrations ($C_m = 0$–3.0%), mainstream mean velocities ($U_p = 0.5$–5.0 m/s) and side-stream velocities ($U_j = 1.0$–12.7 m/s). A modified mixing index was used to quantify the mixing. The mixing behavior in the presence of fibers differed significantly from that in water flow. At a specific jet-to-pipe diameter ratio, the jet-to-pipe velocity ratio was the main parameter determining the mixing quality in the water flow. For suspension flow, however, both main stream velocity and jet penetration were major factors, due to the complex rheology of the pulp suspensions and flow regimes. This article extends the previous work to examine the effect of injection tube length, flow regime, jet penetration, and fiber properties on mixing quality, and to develop criteria for optimizing in-line jet mixing in pulp suspensions.

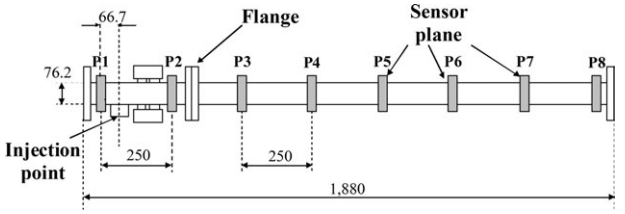

Figure 1. Schematic of test section (with all dimensions in mm).

Experimental

The equipment in this study was described in detail by Yenjaichon et al.[1] A test section, 76.2 mm diameter and 1.88 m long, featuring eight 16-electrode sensor planes at 0.25 m intervals, was installed 5 m downstream of a pipe bend in a pilot-scale flow loop facility to provide fully developed flow before entering the test section. For each sensor plane, 16 circular stainless steel electrodes of diameter 6.35 mm were spaced uniformly around the vessel periphery. As shown in Figure 1, the side-stream injection point for aqueous NaCl solution was located between the first and second sensor planes. An ITS P2000 ERT system (Manchester, UK) acquired the data, with image reconstruction based on a linear back-projection algorithm.

Steady-state experiments were conducted with constant mainstream and side-stream flow rates. The tracer concentration varied from 0.9 to 2.4 g/L. The temperature in the main stream was maintained at 20 ± 5°C, while the temperature difference between the main and side streams was always less than 10°C. The hardwood pulp in this study was bleached Maple kraft pulp, with fibers 0.60 mm in length, 16.6 μm in diameter, and 0.066 mg/m in coarseness on average. The softwood pulp was Northern Bleached Softwood Kraft pulp from Canfor Pulp Ltd., Prince George, BC, with fibers 2.52 mm long, 27.6 μm in diameter, and 0.129 mg/m in coarseness on average.

The modified mixing index (M') derived by Yenjaichon et al.[1] is used to quantify the mixing quality. It is determined from the individual conductivity values from each image pixel (316 in each cross-sectional plane).

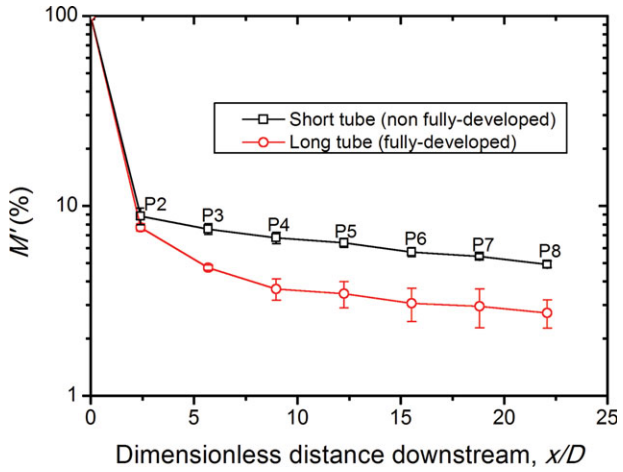

Figure 2. Comparison of long and short injection tubes on modified mixing index at U_p = 1.0 m/s, U_j = 2.0 m/s, D_r = 0.167 for fiber-free water.

P followed by a number designates sensor plane shown in Figure 1. [Color figure can be viewed in the online issue, which is available at wileyonlinelibrary.com.]

$$M' = \frac{\sqrt{M_m^2 - M_S^2}}{M_{FS}} \tag{4}$$

where

$$M_m = \frac{\sigma}{\bar{y}} = \frac{\sqrt{\frac{\sum_{i=1}^{n}(y_i - \bar{y})^2}{n-1}}}{\bar{y}} \tag{5}$$

and

$$M_{FS} = \frac{\sqrt{Q_p Q_j}}{Q_j C_j + Q_p C_p} |C_p - C_j| \tag{6}$$

M_m is the mixing index measured under the given test conditions, M_{FS} the mixing index for fully segregated flow at the same mean concentration and M_s the system mixing index in the absence of tracer (brine solution). σ is the standard deviation of the conductivity values, y_i the local mixture conductivity determined from ERT measurements, $\bar{y}$ the average conductivity, and n the total number of pixels in the measurement plane. C_p is the salt concentration in the main stream or pipe flow, C_j the salt concentration in the side stream for jet flow, Q_p the volumetric flow rate of the main stream, and Q_j the volumetric flow rate of the side stream. The modified mixing index is 100% for fully segregated flow. As the mixing improves, M' decreases, approaching 0 for perfect mixing.

Results and Discussion

Effect of injection tube length on mixing quality

Figure 2 shows the effect of injection tube length on mixing quality for the same mainstream and side-stream velocities. Error bars in this and subsequent figures correspond to 90% confidence intervals. The entrance length was approximately $24D_j$ for a jet velocity, U_j, of 2.0 m/s and a jet Reynolds number, Re_j, of 25,710. The longer injection tube length was sufficiently long (length: diameter ratio, L_j/D_j, of 36), to provide fully developed turbulent flow, whereas the flow was not fully developed for the short tube (L_j/D_j = 14). The modified mixing index for the fully developed flow was significantly lower for the non-fully developed one, suggesting better mixing when the side-entering jet was fully developed. Tomographic images for the same condition are shown in Figure 3. Due to misalignment between the actual electrode position and the electrode position in the ERT reconstruction process, the top position of the pipe in the tomographic image is rotated counterclockwise by 11° from the vertical axis, and a corresponding corrective rotation was applied to all images obtained in this study. From the tomographic images, the high-conductivity region in red and yellow represents the brine solution injected into the system, whereas the low-conductivity region in blue represents the main stream. The tracer was injected between planes 1 and 2. Mixing quality improved along the pipe, as seen from the disappearance of the red and yellow colors from plane 2 to plane 8. The fully developed side-stream flow penetrated further into the main pipe than the developing one since the velocity profile was flatter when the flow was not yet fully developed. Further penetration of the jet stream into the main stream provided better downstream mixing. Long injection tubes were therefore used for all subsequent tests.

Effect of temperature and jet penetration on mixing quality in water flow

All tests were in the turbulent flow regime for both the main stream (Re_p = 38,100–381,000) and jet stream (Re_j = 9,750–48,600). The temperature was varied from 15 to 25°C, changing the viscosity of the water by 22%. However, the Reynolds number was high enough that the dependence of mixing quality on Reynolds number, and hence on liquid

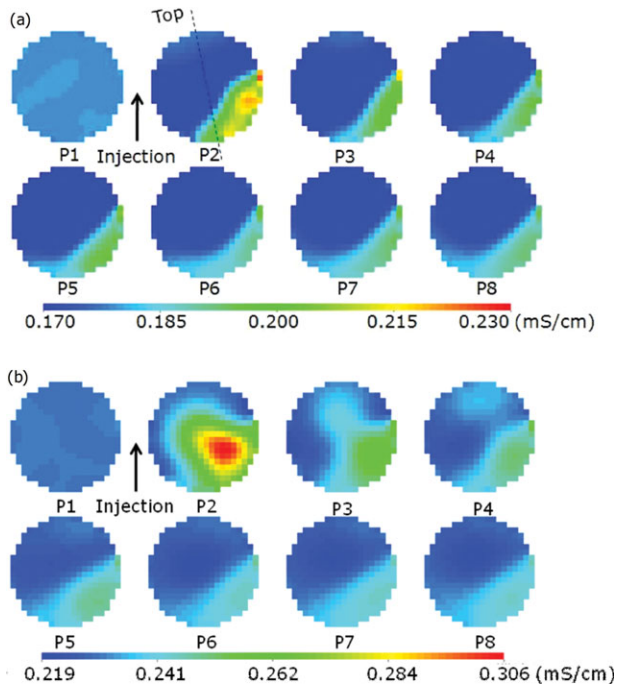

Figure 3. Tomographic images for water flow at U_p = 1.0 m/s, U_j = 2.0 m/s, D_r = 0.167: (a) short injection tube; (b) long injection tube.

The locations of planes P1 to P8 are shown in Figure 1. [Color figure can be viewed in the online issue, which is available at wileyonlinelibrary.com.]

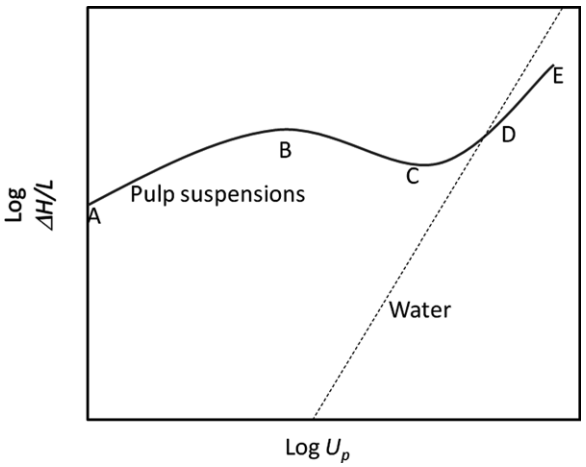

Figure 4. Typical head loss-velocity curve for water and low consistency pulp-suspension flow through pipes.

Line AE is derived from Robertson and Mason[24] for pulp suspensions. Dashed line is the corresponding line for water.

viscosity, was negligible. On the other hand, the mixing quality for the Newtonian fluid (water) in the turbulent flow was strongly dependent on the jet penetration, and thus on the jet-to-pipe velocity ratio. The mixing quality improved significantly with increasing jet-to-pipe velocity ratio as the mixing mode changed from wall-source to jet-mixing and jet-impaction, with improving mixing quality for each respective mixing mode as described previously.[1] At low velocity ratios ($R < 4$), the jet rapidly bent and attached to the near wall, so that the degree of mixing was poor. As the velocity ratio increased ($4 \leq R \leq 10$), the jet penetrated to the pipe axis and joined the main flow, causing the mixing to improve significantly. At even higher velocity ratios ($R > 10$), the jet impinged on the far wall, then spreading circumferentially over the pipe inner periphery, with better mixing downstream.

Flow regime of hardwood pulp suspension flow in pipe

For flow of pulp suspensions in pipes, it is customary to identify the flow regime as plug, mixed or turbulent, based on criteria suggested by Robertson and Mason.[24] Figure 4 shows a typical logarithmic head loss-velocity curve for flow of a low consistency pulp suspension through pipes. At very low velocity in region AB (referred to as "plug flow"), the suspension travels like a piston. This region is called the plug flow regime. In region BC, an annular water layer in laminar flow surrounds the plug, with this layer becoming turbulent at point C. At higher velocity in region CD, turbulent stresses in the water layer degrade the plug, and fibers begin to move into the thin turbulent annulus. The fibers in the water annulus suppress turbulence, reducing momentum transport and leading to less friction loss in the suspension than in water, referred to as the onset of drag reduction.[25] A plug persists throughout BD, with its size decreasing with increasing velocity until the plug disappears and the flow becomes turbulent at point E.

Figure 5 illustrates the head loss curve for the hardwood kraft pulp. The flow could be either plug or turbulent, depending on the mainstream velocity. At $C_m = 1.0\%$, the flow was essentially plug in the mixed flow regime for $U_p \leq 2.0$ m/s, and became turbulent at $U_p \geq 3.0$ m/s. The friction loss in the suspension became less in water at $U_p \cong 1.0$ m/s, likely due to the fibers in the annular water layer dampening turbulence. At the highest fiber mass concentration ($C_m = 3.0\%$), however, the flow was essentially plug, with more friction loss than in water for all mainstream velocities investigated (0.5–5.0 m/s).

Effect of velocities on mixing quality for hardwood and softwood pulp

The jet mixing behavior of softwood and hardwood pulp suspensions was found to be very similar. The flow regime was important in determining the mixing quality for both pulp types. Figure 6 shows the effect of the mainstream velocity on the mixing quality for the hardwood pulp suspension at $C_m = 1.0$ and 3.0% for the same diameter ratio and almost the same jet-to-pipe velocity ratio. At $C_m = 1.0\%$, the results were very similar to those for softwood pulp suspension at $C_m = 0.5\%$.[1] Increasing the mainstream velocity changed the flow regime from mixed flow (at $U_p \leq 2.0$ m/s) to the turbulent flow regime (at $U_p \geq 3.0$ m/s), resulting in plug disintegration and significantly better mixing, approaching that of the corresponding water flow, as shown in Figure 6a. At a higher mass concentration ($C_m = 3.0\%$), however, (Figure 6b) the mainstream velocity had little effect on the mixing quality. The degree of mixing was poor, with only a slight increase in mixing quality observed with increasing mainstream velocity, as the fiber networks were robust and the suspension remained in plug flow for all mainstream velocities tested.

Jet velocity is another important factor influencing mixing quality. The mixing behavior was again similar for hardwood and softwood pulp suspensions. Figure 7 portrays the effect of jet velocity on mixing for hardwood pulp suspensions for $U_p = 0.5$ m/s and $D_r = 0.05$. For dilute hardwood pulp suspensions ($C_m \leq 1.0\%$), the mixing quality depended strongly on the jet velocity. Mixing improved significantly with increasing jet velocity at $C_m = 1.0\%$, as shown in Figure 7a. At $C_m = 3.0\%$ (Figure 7b), the mixing quality depended on the jet penetration into the pipe. The mixing quality was poor when the jet attached to the wall of the pipe (far wall at $R = 12.3$ and near wall at $R = 24.1$);

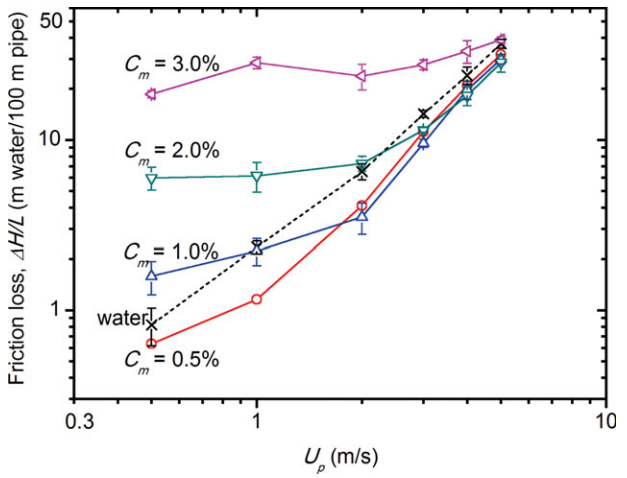

Figure 5. Head loss-velocity curves for water and hardwood kraft pulp.

[Color figure can be viewed in the online issue, which is available at wileyonlinelibrary.com.]

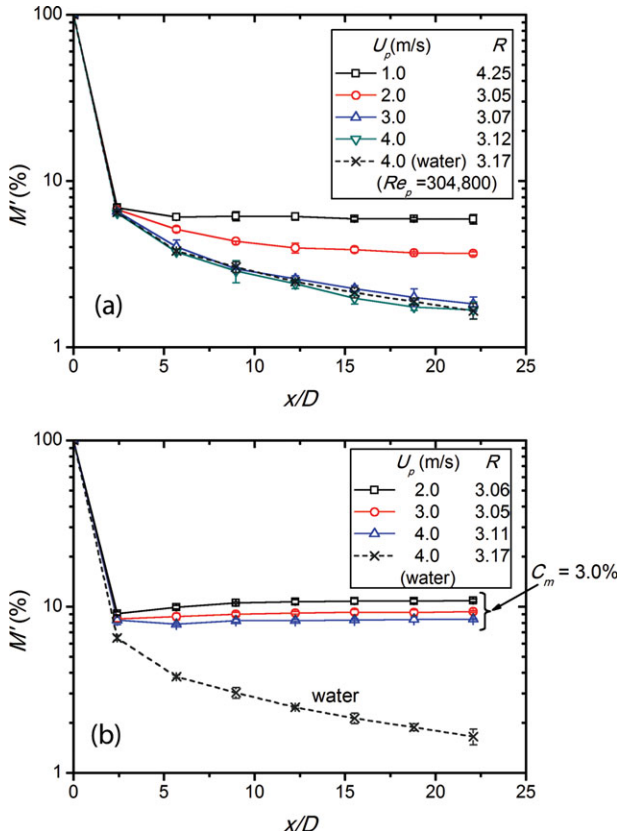

Figure 6. Modified mixing index as a function of dimensionless distance downstream at different fiber mass concentrations of hardwood pulp suspensions: (a) C_m = 1.0% and (b) C_m = 3.0% for D_r = 0.05, almost identical jet-to-pipe velocity ratios and various mainstream velocities, and comparison with modified mixing index for water under very similar experimental conditions.

[Color figure can be viewed in the online issue, which is available at wileyonlinelibrary.com.]

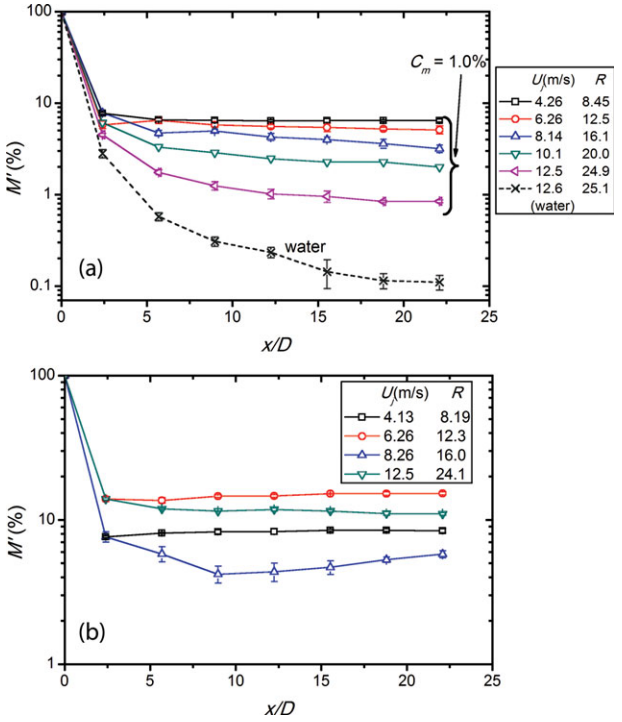

Figure 7. Modified mixing index as a function of dimensionless distance downstream at different fiber mass concentrations of hardwood pulp suspensions: (a) C_m = 1.0% and 0% and (b) C_m = 3.0% for U_p = 0.5 m/s, D_r = 0.05 and various jet velocities.

[Color figure can be viewed in the online issue, which is available at wileyonlinelibrary.com.]

the mixing was better when the jet penetrated to the core of the pipe (R = 8.19). The mixing was optimal at R = 16.0 when the jet impinged on the far wall and circulated back to the core of the pipe. The data consistently showed this behavior for $C_m \geq 2.0\%$ (hardwood pulp) and $C_m \geq 1.0\%$ (softwood pulp). However, the jet velocities or velocity ratios required for optimum mixing depended on the mass concentrations due to different fiber network strength, with higher velocity ratios needed for higher mass concentrations. The optimum values are summarized in Table 1.

Decaying turbulence likely occurred at R = 16.0 as shown in Figures 7b and 8c. Energy dissipation from the jet impaction disrupted the fiber networks, and mixing quality improved for the first three planes (P2–P4) downstream of the injection point as shown in Figure 7b. However, reflocculation probably occurred downstream, since the energy dissipation required to maintain turbulence was not sustained, causing the mixing quality to worsen downstream. With the downstream reflocculation, a plug formed at the center of the pipe, pushing the brine solution toward the pipe wall. This can be seen from the formation of the high-conductivity regions in red and yellow around the pipe, especially at the top of the P8 image in Figure 8c. This explanation also applies at R = 12.3 where the jet again disrupted the plug and reached the far wall of the pipe, with reflocculation downstream. For R = 8.19, however, the tracer did not reach the opposite pipe wall since the jet fluid joined the main flow in the core of the pipe and travelled with the plug.

In addition to mass concentration, the jet velocity (or velocity ratio) required for the jet to reach the axis of the pipe is a function of the mainstream velocity as the fiber network strength depends on the mainstream velocity. At the same mass concentration, a higher velocity ratio is needed for lower mainstream velocity due to stronger fiber networks. This differs from the behavior in water flow, as the velocity ratio required for the jet to reach the center of the pipe is almost independent of the mainstream velocity. The velocity ratios required for the jet to penetrate to the center of the pipe for different pulp types, mass concentrations, and

Table 1. Velocity Ratios for Optimum Mixing at U_p = 0.5 m/s, D_r = 0.05

Pulp Type	Fiber Mass Concentration, C_m (%)	Optimum Velocity Ratio
Softwood	1.0	10–14*
	2.0	16.9
	3.0	19.7
Hardwood	2.0	12–15*
	3.0	16.0

*Approximate; clearly between these two limits.

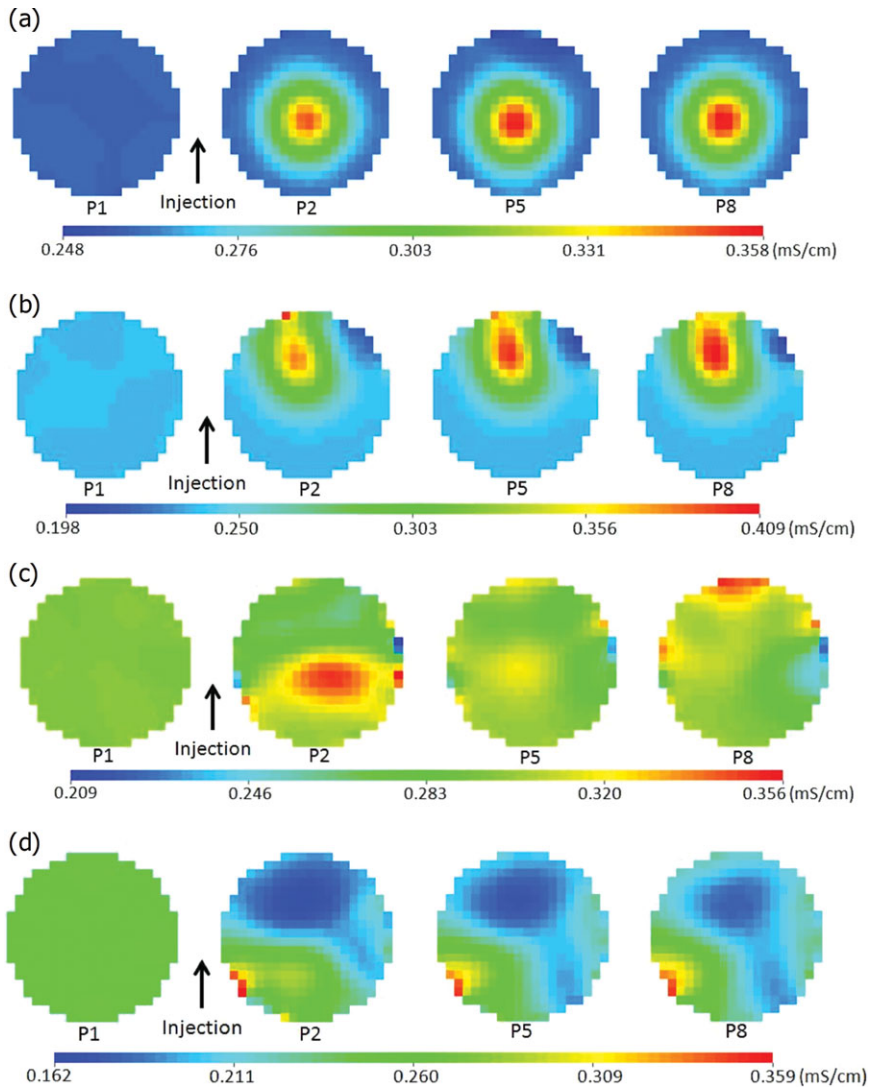

Figure 8. Tomographic images for hardwood pulp suspension flow at U_p = 0.50 m/s for C_m = 3.0%, D_r = 0.05 at: (a) R = 8.19; (b) R = 12.3; (c) R = 16.0; and (d) R = 24.1.

The locations of planes P1, P2, P5 and P8 are shown in Figure 1.

mainstream velocities are summarized in Table 2. Due to a limitation of the liquid injection system, data could only be obtained for $U_p \leq 2.0$ m/s. At $U_p = 2.0$ m/s, the required velocity ratio for the jet to penetrate to the axis of the pipe approached that for water, except for 3.0% softwood pulp suspension where the required velocity ratio was slightly higher than that for water, suggesting that the effect of fiber network strength became less significant at this mainstream velocity. At higher velocities ($U_p \geq 2.0$ m/s), therefore, the required velocity ratio also likely approaches that for water for the fiber mass concentration range investigated. Although the velocity ratios for optimum mixing in Table 1 are useful indicators, they are not necessarily desirable from a practical point of view since impingement on the pipe wall creates significant stress there. At higher mass concentrations ($C_m \geq$ 2.0% for hardwood pulp suspension and $C_m \geq 1.0\%$ for softwood pulp suspension), the mixing quality was poor when the jet attached to the pipe wall, and the design criteria can thus be based on the velocity ratio for the jet to reach the axis of the pipe, as shown in Table 2.

Effect of fiber-turbulence interactions on mixing quality for hardwood pulp

Figure 9 shows the effect of the mainstream velocity on mixing quality for a hardwood pulp suspension with $C_m = 0.5\%$ at virtually identical jet-to-pipe velocity ratio and identical diameter ratio. The suspension flow was clearly in the turbulent regime for all mainstream velocities examined, and the mixing quality in hardwood suspension flow was somewhat better than that for water without fibers. The slight increase in mixing quality at a lower velocity ($U_p = 2.0$ m/s) was likely due to the longer retention time. Figure 10 compares the hardwood suspension at $C_m = 0.5\%$ and water flow at $U_p = 3.0$ m/s for various jet velocities. Mixing quality improved with increasing velocity ratio, with consistently better mixing quality for the dilute hardwood suspension than for water in the turbulent flow regime. However, mixing quality was worse for the softwood suspension at the same fiber mass concentration in the turbulent flow regime, as shown in Figure 11. This might be due to the longer fibers creating stronger fiber networks for the softwood than for the hardwood,

Table 2. Velocity Ratios for Jet Reaching Center of Pipe for $D_r = 0.05$

Fluid	Fiber Mass Concentration, C_m (%)	Mainstream Velocity, U_p (m/s)	Velocity Ratio for Jet Reaching Axis of Pipe
Water	–	–	6.2
Softwood	0.5	0.5	<8.0*
		1.0	6.0
		2.0	6.3
	1.0	0.5	7.7
		1.0	6.2
		2.0	6.3
	2.0	0.5	9.6
		1.0	7.7
		2.0	6.4
	3.0	0.5	11.0
		1.0	8.3
		2.0	>6.3*
Hardwood	0.5	0.5	<8.0*
		1.0	6.2
		2.0	6.2
	1.0	0.5	<8.0*
		1.0	6.2
		2.0	6.2
	2.0	0.5	8.2
		1.0	6.3
		2.0	6.2
	3.0	0.5	9.0
		1.0	8.1
		2.0	6.2

*Unable to obtain due to limitation of liquid injection system.

thereby, suppressing turbulent fluctuations and hence mixing. Another factor could be increased resistance to bending of the larger-diameter softwood fibers when subjected to flow-induced stresses, affecting the extent to which the two types of fibers dampen turbulence. The differences in the mixing quality are relatively small, but significant, as error bars for each curve seldom overlap each other.

The improved mixing for the short-fiber hardwood pulp suspension coincides with results reported by Luettgen et al.,[6] who also found that turbulent dispersion was greater for a dilute hardwood suspension (at $C_m = 0.5\%$) than for fiber-free water. The results also agree with findings summarized by Bobkowicz and Gauvin,[2,3] who reported that the radial intensity of turbulence in water flow containing short nylon fibers (of length from 0.52 to 1.21 mm) was higher than that for water without fibers, even though the suspension flow was in the drag reduction regime. It is generally believed that drag reduction is due to the suppression of turbulent eddies by fibers or other particles. Several studies[26–30] have suggested that drag reduction in fiber suspensions is especially due to dampening of radial velocity fluctuations in the turbulent core, in contrast to drag reduction in polymer

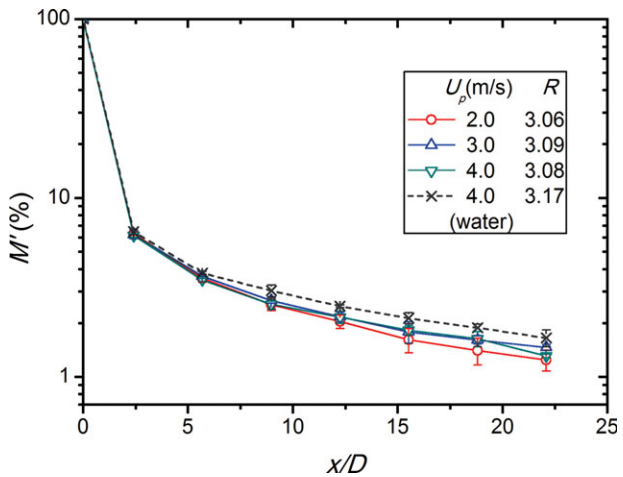

Figure 9. Modified mixing index as a function of dimensionless distance downstream for hardwood pulp suspension at $C_m = 0.5\%$, $R = 3.1$ compared with water for various mainstream velocities and almost identical jet-to-pipe velocity ratios.

[Color figure can be viewed in the online issue, which is available at wileyonlinelibrary.com.]

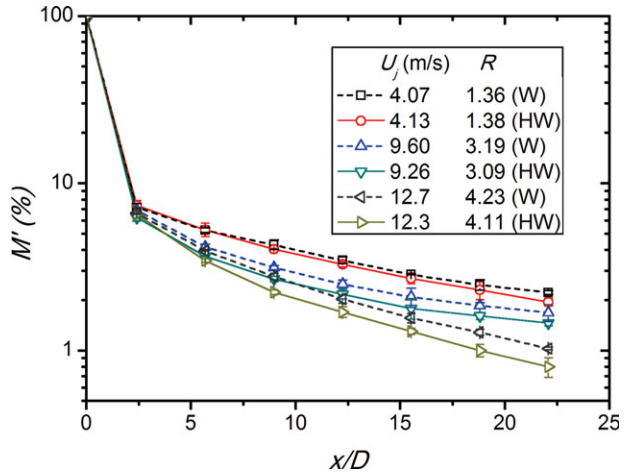

Figure 10. Modified mixing index as a function of dimensionless distance downstream for water (W) and hardwood pulp suspension (HW) flow at $C_m = 0.5\%$, $U_p = 3.0$ m/s with various jet velocities.

[Color figure can be viewed in the online issue, which is available at wileyonlinelibrary.com.]

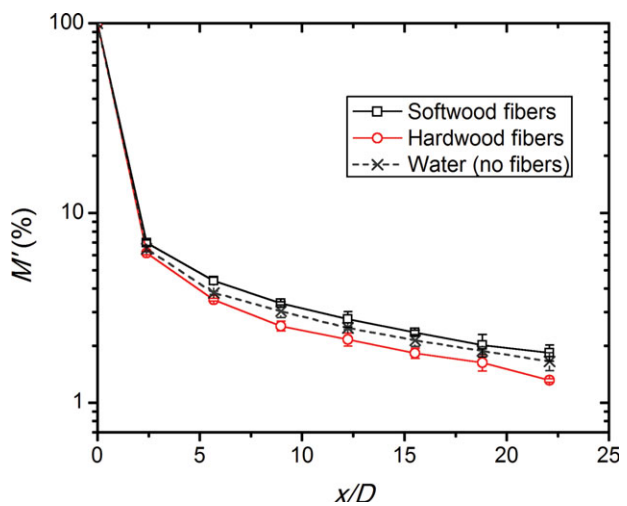

Figure 11. Modified mixing index as a function of dimensionless distance downstream for water, softwood and hardwood pulp suspensions at $C_m = 0.5\%$, $U_p = 4.0$ m/s, $R = 3.1$ and $D_r = 0.05$.

[Color figure can be viewed in the online issue, which is available at wileyonlinelibrary.com.]

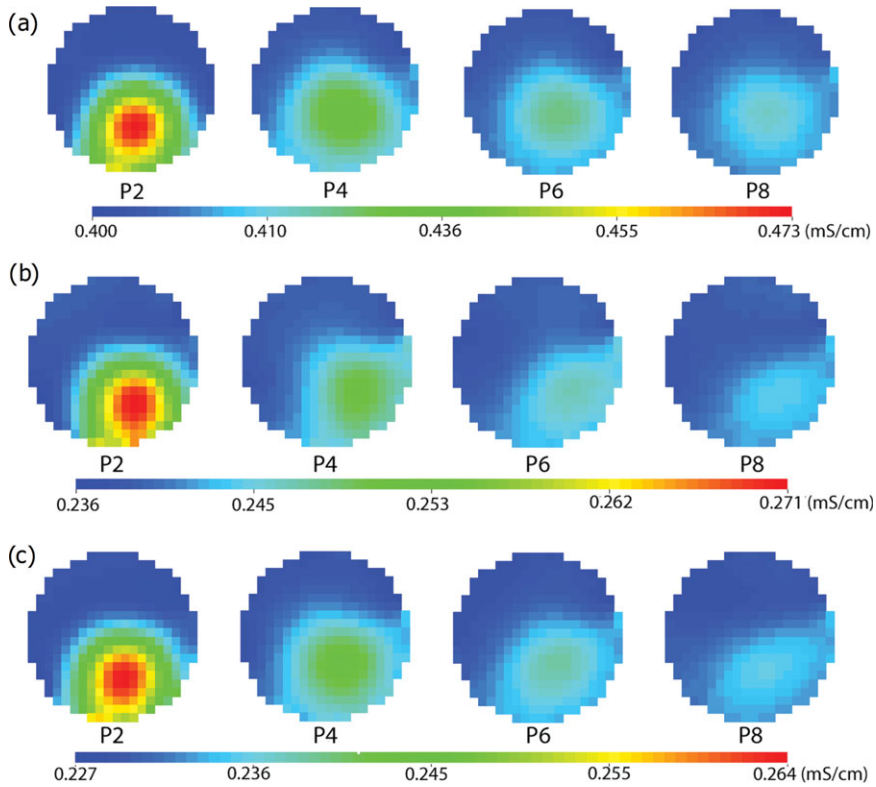

Figure 12. Tomographic images for C_m = 0.5%, U_p = 4.0 m/s, R = 3.1 and D_r = 0.05 with: (a) softwood; (b) hardwood; and (c) fiber-free water.

The locations of planes P2, P4, P6 and P8 are shown in Figure 1. [Color figure can be viewed in the online issue, which is available at wileyonlinelibrary.com.]

solutions, in which drag reduction is due to dampening near the wall.[31,32] This implies less turbulent dispersion and reduced lateral mixing, which appears to contradict the experimental results of improved mixing for the hardwood fibers. However, fiber aspect ratios in those previous studies were relatively high (>70), close to that for the softwood fibers (92), and significantly higher than that for the hardwood fibers (36) in this study. A softwood suspension likely forms fiber networks, dampening turbulent fluctuation in the core, whereas a short-fiber hardwood suspension probably behaves differently.

The crowding number, N_c, of 123, calculated from Eq. 3 for the 0.5% softwood suspension, significantly exceeded the critical value of 60, indicating more than three contacts per fiber. Consequently, fibers entangled, flexed, and formed networks from frictional forces between them in the bent configuration.[13] In the turbulent fiber suspension flow, these networks were in a dynamic equilibrium between simultaneous floc formation and breakdown of flocs by shear stress,[24] and likely suppressed turbulent dispersion in the core of the suspension flow, leading to less momentum transport than in water flow and hence to drag reduction. For the hardwood, the crowding number of 13.8 for C_m = 0.5% was lower than the gel crowding number of 16. Accordingly, fibers were free to move relative to one another. Individual fibers were then free to migrate throughout the main flow, and the mechanism of drag reduction possibly differed from that for softwood fibers. The changes in turbulence structure causing drag reduction in hardwood fibers probably occur only in the wall layer, as for drag-reducing polymeric fluids. Improved turbulent dispersion over the entire cross-section of the pipe is therefore compatible with drag-reducing flow.

Figure 12 compares tomographic images for water (C_m = 0) with C_m = 0.5% softwood and hardwood suspensions for the same flow conditions in the turbulent flow regime. Similar jet penetration was observed at P2 for each case. The distribution and disappearance of high conductivity regions in the hardwood suspension were similar to those in water, but differed from those in the softwood suspension, as shown from the image contours downstream, especially at P6 and P8. The drag reduction mechanism for the hardwood fibers therefore probably differed from that for the softwood fibers. Due to high number of fiber contacts in the softwood suspension suggested by the crowding number, floc formation likely suppressed turbulence in the core of the pipe, consistent with the high-conductivity region being concentrated further from the pipe wall at P6 and P8. In the hardwood fibers with lower crowding, however, the tracer spread near the pipe wall, indicating negligible floc formation occurring in the core, and turbulence was probably dampened in the near-wall region.

Accordingly, drag reduction in hardwood suspensions might not be a determining factor for the overall mixing quality as it is predominantly related to near-wall behavior, whereas mixing in our study was measured over the entire pipe cross-section. This implies that short fibers might alter the turbulence structure in the bulk, leading to better mixing in hardwood suspensions than in fiber-free water. The crowding number for the hardwood fibers suggested that the

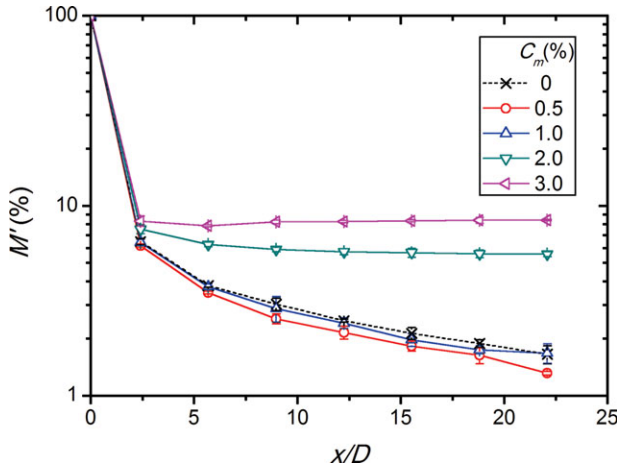

Figure 13. Modified mixing index as a function of dimensionless distance downstream for hardwood pulp suspensions at U_p = 4.0 m/s, R = 3.1 with various fiber mass concentrations.

[Color figure can be viewed in the online issue, which is available at wileyonlinelibrary.com.]

suspensions behaved as essentially dilute, with individual fibers moving free of one another throughout the flow, possibly carrying turbulent eddies with them. Fibers may also have collided with each other, generating local turbulent eddies. These factors could promote turbulent dispersion, resulting in improved mixing in a dilute hardwood suspension.

McComb and Chan[33] reported that the longitudinal component of turbulent velocity fluctuations in fiber suspension flow decreased, whereas the tangential component increased, relative to water flow. An increase in tangential fluctuations could promote turbulent dispersion and mixing quality. Luettgen et al.[6] proposed that the motion of flocs in the suspension flow provided a mechanism for increasing longitudinal and tangential velocity fluctuations, while suppressing radial fluctuations, and proposed that this mechanism could promote turbulent dispersion in drag-reducing flow.

Figure 13 plots the modified mixing index for various fiber mass concentrations at U_p = 4.0 m/s. The results show the effects of flow regime and fiber-turbulence interactions on the mixing quality. Plug flow was approached at $C_m \geq$ 2.0%, leading to poor mixing downstream. At lower mass concentrations ($C_m \leq$ 1.0%), the flow was in the turbulent regime, and the mixing quality was much better. Better mixing quality than for water occurred at C_m = 0.5% but not at C_m = 1.0%. The crowding number was 13.8 for C_m = 0.5%, whereas it was 27.6 for C_m = 1.0%. The latter was higher than the gel crowding number of 16, causing fibers to interact and begin to flocculate. It appears that the fiber mass concentration needs to be sufficiently high for fiber-turbulence interactions to improve dispersion, but not be so high as to engender fiber networks strong enough to reduce turbulent fluctuations.

Effect of fiber type on mixing quality

Figure 14 shows the effect of fiber type on mixing at U_p = 3.0 m/s. The mixing quality for the short-fiber hardwood pulp suspension was substantially better than for the softwood suspension, and was very similar to that for water, as illustrated in Figure 14a. At this consistency and mainstream velocity, the turbulent shear was sufficient to disrupt the fiber networks for hardwood suspension, causing the flow to become turbulent, leading to enhanced mixing. For the same conditions, the fiber networks for softwood suspension were robust, flowing as a plug, resulting in poor mixing. However, the fiber properties did not have such a strong effect on mixing quality at the higher mass concentration of 3.0%, as indicated in Figure 14b. In this case, mixing was similar for both fiber types, and poor relative to water, as plug flow occurred in both cases.

Conclusions

For mixing in water, the mixing quality for a long injection tube providing fully developed jet flow was significantly better than that for a short one due to the flatter velocity profile of developing flow causing less jet penetration. Temperature between 15 and 25°C had insignificant effect on the mixing quality.

Mixing quality was significantly worse for suspensions in the plug and mixed flow regimes than in turbulent flow, due

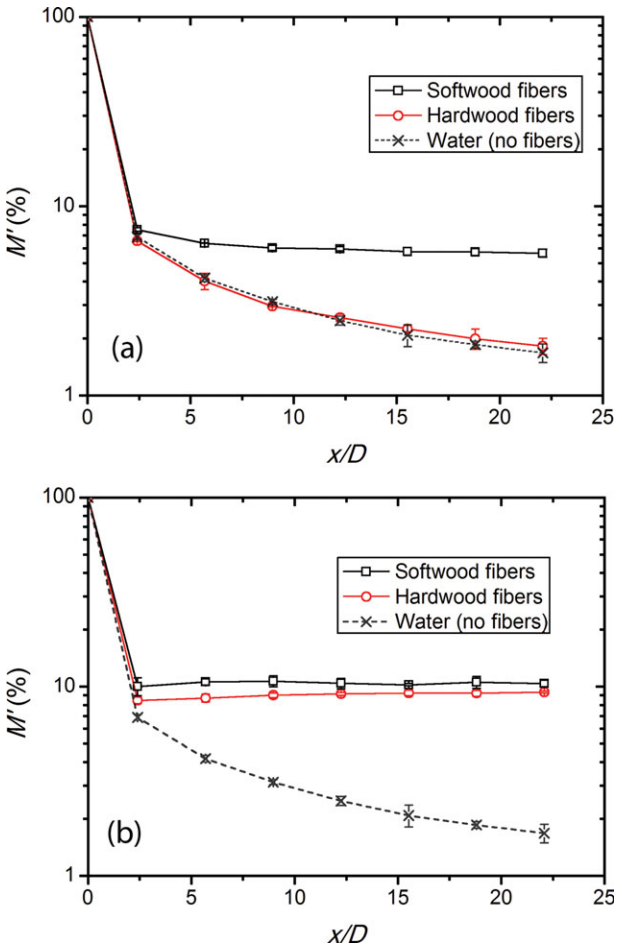

Figure 14. Modified mixing index as a function of dimensionless distance downstream for water, softwood and hardwood pulp suspensions at (a) C_m = 1.0% and (b) C_m = 3.0%, for U_p = 3.0 m/s and R = 3.1.

[Color figure can be viewed in the online issue, which is available at wileyonlinelibrary.com.]

to strong fiber networks of the core plug suppressing dispersion. In turbulent flow, mixing behavior for both softwood and hardwood pulps was similar to that for water. For a given jet-to-pipe diameter ratio, the mixing was almost independent of the mainstream velocity at the same jet-to-pipe velocity ratio. Mixing improved with increasing ratio of injection velocity to mainstream velocity for a constant jet-to-pipe diameter ratio.

For plug flow in the mixed flow regime with a loose fiber network, the jet could disrupt the plug. Mixing improved with increasing jet velocity, but was significantly lower than for water for $C_m = 0.5\%$ with softwood pulp, and for $C_m \leq 1.0\%$ with hardwood fibers. However, at higher fiber mass concentrations, the mixing quality depended on jet penetration. Jet attachment to the far wall of the pipe led to poor mixing. Mixing quality improved when the jet penetrated to the axis of the pipe, and improved further when the jet impinged on the opposite wall and then recirculated to the core of the pipe. Higher jet velocities were required for the jet to penetrate to the center of the pipe at higher mass concentrations and lower mainstream velocities due to denser fiber networks.

In the turbulent flow regime, the mixing for a dilute hardwood suspension at $C_m = 0.5\%$ was somewhat better than for water, whereas it was worse for a softwood suspension at the same concentration. Drag reduction may not be directly linked to the overall degree of mixing in hardwood suspensions as it predominantly reflects behavior in the wall layer. Shorter smaller-diameter fibers likely modify the turbulence structure in the bulk, resulting in better mixing over the entire pipe cross-section, whereas high mass concentration and long large fibers create fiber networks that reduce turbulent fluctuations and mixing quality.

Acknowledgments

The authors thank NSERC, FPInnovations (Paprican Division), and Howe Sound Pulp and Paper Ltd. for their support. The authors are also grateful to Dr. Richard Kerekes for technical assistance, and Drs. James Olson and Mark Martinez for providing access to the flow loop facility.

Notation

C_j = salt concentration in side stream or jet flow, kg/m^3
C_m = suspension mass concentration or consistency, %
C_p = salt concentration in main stream or pipe flow, kg/m^3
C_v = suspension volumetric concentration
d = fiber diameter, m
D = pipe diameter, m
D_j = injection tube diameter, m
D_r = jet-to-pipe diameter ratio
L = fiber length, m
L_j = injection tube length, m
M_{FS} = mixing index for fully segregated flow defined by Eq. 6, %
M_m = measured mixing index defined by Eq. 5, %
M_s = system mixing index measured in absence of tracer, %
M' = modified mixing index defined by Eq. 4, %
N_c = crowding number defined by Eq. 3
Q_j = volumetric flow rate of side stream, m^3/s
Q_p = volumetric flow rate of main stream, m^3/s
n = number of image pixels
R = jet-to-pipe mean velocity ratio, i.e., U_j/U_p
Re_j = jet Reynolds number
Re_p = pipe Reynolds number
U_p = mainstream or pipe velocity, m/s
U_j = side-stream or jet velocity, m/s
x = distance downstream of injection, m
y_i = local mixture electrical conductivity, mS/cm
$\bar{y}$ = average electrical conductivity, mS/cm

Greek letters

$\Delta H/L$ = friction loss, m water/100 m pipe
σ = standard deviation of conductivity in tomographic image, mS/cm
ω = fiber coarseness, kg/m

Literature Cited

1. Yenjaichon W, Grace JR, Lim CJ, Bennington CPJ. In-line jet mixing of liquid-pulp-fibre suspensions: effect of concentration and velocities. *Chem Eng Sci*. 2012;75:167–176.
2. Bobkowicz AJ, Gauvin WH. The turbulent flow characteristics of model fibre suspensions. *Can J Chem Eng*. 1965;43:87–91.
3. Bobkowicz, AJ, Gauvin WH. The effects of turbulence on the flow characteristics of model fibre suspensions. *Chem Eng Sci*. 1967;22:229–241.
4. Andersson O. Some observations on fibre suspensions in turbulent motion. *Svensk Papperstid*. 1966;69:23–31.
5. Luthi O. *Pulp rheology applied to medium consistency pulp flow. Proceedings of the 1987 TAPPI Engineering Conference*. Atlanta, GA, 1987:347–353.
6. Luettgen CO, Lindsay JD, Stratton RA. Turbulent dispersion in pulp flow: preliminary results and implications for the mechanisms of fiber-turbulence interactions. *IPST Tech Pap Ser*. 1991;408:1–29.
7. Rewatkar VB, Kerekes RJ, Bennington CPJ. Use of temperature profiling to measure mixing quality in pulp bleaching operations. *Pulp Pap Can*. 2002;103:T173–T179.
8. Kerekes RJ. Rheology of fibre suspensions in papermaking: an overview of recent research. *Nord Pulp Pap Res J*. 2006;21:100–114.
9. Mason SG. The motion of fibres in flowing liquids. *Pulp Pap Mag Can*. 1950:93–100.
10. Kerekes RJ, Soszynski RM, Tam Doo PA. *The flocculation of pulp fibres. Transactions of the 8th Fundamental Research Symposium*. Oxford, 1985, 265–310.
11. Soszynski RM. The formation and properties of coherent flocs in fibre suspensions, PhD Dissertation. The University of British Columbia, 1987.
12. Kerekes RJ, Schell CJ. Characterization of fibre flocculation regimes by a crowding factor. *J Pulp Pap Sci*. 1992;18:J32–J38.
13. Meyer R, Wahren R. On the elastic properties of three-dimensional fibre networks. *Svensk Papperstid*. 1964;67:432–436.
14. Martinez DM, Buckley K, Jivan S, Lindstrom A, Thiruvengadaswamy R, Olson JA, Ruth TJ, Kerekes RJ. *Characterizing the mobility of papermaking fibres during sedimentation. Transactions of the 12th Fundamental Research Symposium*. Oxford, 2001, 225–254.
15. Celzard A, Fierro V, Kerekes RJ. Flocculation of cellulose fibres: new comparison of crowding factor with percolation and effective-medium theories. *Cellulose* 2009;16:983–987.
16. Simmons MJH, Edwards I, Hall JF, Fan X, Parker DJ, Stitt EH. Techniques for visualization of cavern boundaries in opaque industrial mixing systems. *AIChE J*. 2009;55:2765–2772.
17. Hosseini S, Patel D, Ein-Mozaffari F, Mehrab M. Study of solid–liquid mixing in agitated tanks through electrical resistance tomography. *Chem Eng Sci*. 2010;65:1374–1384.
18. Ishkintana LK, Bennington CPJ. Gas holdup in pulp fibre suspensions: gas voidage profiles in a batch-operated sparged tower. *Chem Eng Sci*. 2010;65:2569–2578.
19. Bhole MR, Hui LK, Gomez C, Bennington CPJ, Dumont GA. The effect of off-wall clearance of a side-entering impeller on the mixing of pulp suspensions in a cylindrical stock chest. *Can J Chem Eng*. 2011;89:985–995.
20. Tahvildarian P, Ng H, D'Amato M, Drappel S, Ein-Mozaffari F, Upreti SR. Using electrical resistance tomography images to characterize the mixing of micron-sized polymeric particles in a slurry reactor. *Chem Eng J*. 2011;172:517–525.
21. Harrison STL, Stevenson R, Cilliers JJ. Assessing solids concentration homogeneity in Rushton-agitated slurry reactors using electrical resistance tomography (ERT). *Chem Eng Sci*. 2012;71:392–399.
22. Yenjaichon W, Pageau G, Bhole M, Bennington CPJ, Grace JR. Assessment of mixing quality for an industrial pulp mixer using electrical resistance tomography. *Can J Chem Eng*. 2011;89:996–1004.
23. Kourunen J, Heikkinen LM, Paananen P, Peltonen K, Käyhkö J, Vauhkonen M. Electrical resistance tomography for evaluating a medium consistency mixer. *Nord Pulp Pap Res J*. 2011;26:179–185.

24. Robertson AA, Mason SG. The flow characteristics of dilute fiber suspensions. *Tappi J*. 1957;40:326–334.
25. Duffy GG, Lee PFW. Drag reduction in the turbulent flow of wood pulp suspensions. *Appita J*. 1978;31:280–286.
26. Lee WK, Vaseleski RC, Metzner AB. Turbulent drag reduction in polymeric solutions containing suspended fibers. *AIChE J*. 1974;20: 128–133.
27. Vaseleski RC, Metzner AB. Drag reduction in the turbulence flow of fiber suspensions. *AIChE J*. 1974;20:301–306.
28. Lee PFW, Duffy GG. Relationships between velocity profiles and drag reduction in turbulent fiber suspension flow. *AIChE J*. 1976;22: 750–753.
29. Lee PFW, Duffy GG. Velocity profiles in the drag reducing regime of pulp suspension flow. *Appita J*. 1976;30:219–226.
30. Sharma RS, Seshadri V, Malhotra RC. Drag reduction in dilute fibre suspensions: some mechanistic aspects. *Chem Eng Sci*. 1979;34: 703–713.
31. Virk PS. Drag reduction fundamentals. *AIChE J*. 1975;21:625–656.
32. McComb WD, Rabie LH. Local drag reduction due to injection of polymer solutions into turbulent flow in a pipe. Part I: dependence on local polymer concentration. *AIChE J*. 1982;28:547–557.
33. McComb WD, Chan KTJ. Laser-Doppler anemometer measurements of turbulent structure in drag-reducing fibre suspensions. *J Fluid Mech*. 1985;152:455–478.

Manuscript received Mar. 22, 2012, and revision received July 6, 2012.